Modelling of turbocharger heat transfer under stationary and transient engine operating conditions

R.D.Burke[1], P. Olmeda[2], F. J. Arnau[2] and M. Reyes-Belmonte[2]
1. Department of Mechanical Engineering, University of Bath, UK
2. CMT – Motores Térmicos, Universitat Politècnica de València, Spain

ABSTRACT

A lumped capacity heat transfer model has been developed and compared to measurements from a turbocharger operating on a 2.2L Diesel engine under steady and transient conditions ranging from 1000-3000rpm and 2-17bar BMEP. The model parameters have been estimated based on similar devices and this study quantifies the errors associated with this approach. Turbine outlet gas temperature prediction was improved with RMSE reduced from 29.5°C to 13°C. A sensitivity study showed the parameters of the heat transfer model influence gas temperatures by only ±4°C but housing temperatures by up to 80°C. Transient simulations showed how errors in the thermal capacitance also lead to errors. This study shows the importance of undertaking a full thermal characterisation and the need for accurate adiabatic maps in turbocharger simulations.

1 INTRODUCTION

The accuracy of turbocharger models needs to increase to allow more use of simulation tools in engine development. Typically heat transfer is ignored in turbocharger models and these are map based, derived from steady state measurements taken on steady flow facilities. A number of studies into the effect of heat transfer have been published over the past 10 years (1-5). The major findings from these investigations are that the heat transfer has a limited effect on the flow behaviour of the turbocharger turbine and compressor, but has a significant influence on the outlet temperatures of the device. On the turbine side heat transfer can represent 20-90% of the total enthalpy drop. Most of this heat is then lost to ambient with the remainder transferred along the bearing housing, primarily to oil and cooling water if present. On the compressor side, the heat transfer is more complex as unless the turbocharger is insulated, heat transfer from the turbine to the compressor is small (6). On the gas stand, as temperature are used to measure work, this gives poor estimates of the aerodynamic performance. When these maps are used on the engine this leads to poor estimation of operating speed, gas temperatures and air flows.

Various models have been proposed to account for heat transfer each employing the assumption that work and heat transfer occur independently in the compressor and turbine. The flow process is therefore split into one or two heat transfers at constant pressure and an adiabatic compression/expansion. Shaaban (3) and Romagnoli and Martinez-Botas (5) provide an analytical solution to heat transfer in the bearing housing simplifying the geometry to a series of cylinders and fit results for an individual device for other model unknowns. Other authors (7, 8) use the lumped capacitance method, splitting the turbocharger housing into a number of thermal nodes linked through convection, conduction and radiation. In this approach, the difficulty lies in determining the thermal resistances between the different nodes. Serrano et al (9) propose a method to calculate conductivities and capacitances using the turbocharger housing as a 1D heat flux probe. They then compare adiabatic, non-adiabatic/externally insulated and non-adiabatic/non-insulated maps to derive the internal convection and external heat losses. In both cases, significant experimental effort on dedicated test facilities is required to parameterise the models. If correctly parameterised, these models offer the potential to reduce exhaust gas temperature prediction errors from +40°C to ±10°C (6). However, in this work the model is applied to a turbocharger operating on an engine system where detailed model parameters were not available.

2 MODEL DESCRIPTION

2.1 Model Overview

An overview of energy flows in turbochargers is shown in figure 1 (a). In addition to work, heat is also transferred between turbine and compressor. This heat can flow to ambient or along the bearing housing towards the cooling oil and further ambient losses. Depending on the operating conditions, heat may continue to be conducted to the compressor housing or, under high compression ratios, this heat flow can reverse.

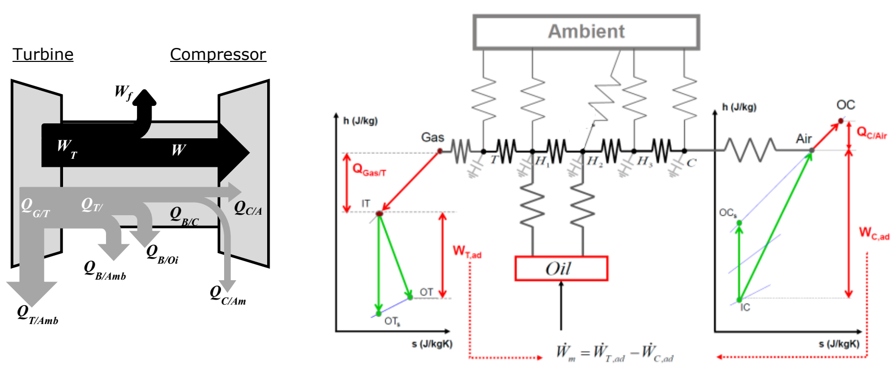

(a) (b)

Figure 1: (a) Work and heat flows in the turbochargers and (b) lumped capacity thermal model

Several studies have demonstrated that radial temperature distribution in a cross sectional area is negligible compared to the axial temperature distribution (10). That evidence allows the simplification of heat transfer problem inside the turbocharger considering it as a one-dimensional problem (9) instead of the three-dimensional case. Figure 1 (b) shows the proposed 1-D lumped model to account for heat transfer effects inside an automotive turbocharger. It includes five metal nodes that are representative for the geometry of the turbocharger. These are T (turbine case), C (compressor case) and three nodes for the turbocharger bearing housing named H1 (placed near turbine case), H2 (placed in the central part, where oil and water comes to the turbocharger) and H3 (placed near compressor case). That division is justified by the high temperature gradient across the housing. Working fluids in turbocharger model have been named from here on as Gas (exhaust gases moving the turbine), Air (compressed air by the compressor), Oil (lubricating oil) and Ambient. In order to simplify the complex heat transfer phenomena in the turbine side and taking into account the exposed areas, it has been assumed that the heat transfer phenomena occurs before the expansion process as it is shown in the left h/s diagram of figure 1 (b). The opposite is true on compressor side and it has been assumed that heat transfer phenomena occurs after the compression work.

Metal nodes are connected by means of conductive conductances ($K_{i,j}$) and the heat flow between two nodes is calculated using Fourier's Law (equation 1). Conductive conductances are represented with thermal resistors drawn in black in figure 1 (b). Conductive conductances between adjacent metal nodes in the turbocharger are constant for any operative condition since that property depends only on the internal geometry and cases material.

$$\dot{Q}_{i,j} = K_{i,j} \cdot \left(T_i - T_j\right) \qquad \mathbf{1}$$

Metal nodes are connected to fluid nodes by means of convective conductances ($hA_{l,i}$) and heat transfer is calculated using Newton's cooling law (equation 2). Connection between metal and fluid nodes is represented by bold grey thermal resistors in figure 1 (b). An additional term for radiation heat transfer is included for the heat transfer between nodes and ambient taking into account the view factors between nodes from simplified geometries (11) (light grey resistors in figure 1 (b)).

$$\dot{Q}_{l,i} = hA_{l,i} \cdot \left(T_l - T_i\right) \qquad \mathbf{2}$$

Metal nodes can store energy during transient processes as their temperature increases or decreases due to their associated mass. That phenomenon has been taken into account in the network model by means of capacitors (represented in light grey). Heat flows in the model are summarised by the following process:

- A proportion of exhaust gases energy is transmitted to the turbine case (node T) before the turbine stator and rotor. This energy ($Q_{Gas/T}$) reduces the temperature governing the expansion process.
- From node T, heat is conducted to node H1 ($Q_{T/H1}$) or transferred to ambient ($Q_{T/AMB}$), or via radiation to nodes H1, H2, H3 and C.
- At node H1, heat flux can be transmitted following these possible paths: conduction to node H2 ($Q_{H1/H2}$), forced convection to oil ($Q_{H1/Oil}$); to ambient ($Q_{H1/AMB}$); or radiation with nodes T and C.
- Node H2 is similar to node H1 for non-water-cooled devices and similar heat flow paths are defined ($Q_{H2/H3}$, $Q_{H2/Oil}$, $Q_{H2/AMB}$ and radiation).

- Housing node H3 in connected by conduction to node C ($Q_{H3/C}$), to ambient ($Q_{H3/AMB}$) and nodes T and C by radiation.
- Compressor node (C) is connected to ambient ($Q_{C/Amb}$), radiation with nodes T, H1, H2 and H3, and by forced convection with a node placed at compressor diffuser ($Q_{C/Air}$).

It is worth noting that for some operative conditions, the temperature after adiabatic compression (node Air) is lower than node C (low loads): in this case the compressed air received heat ($Q_{C/Air}$). At higher loads, the temperature after adiabatic compression can exceed the temperature of node C and this heat flow reverses. Depending on the relative temperatures and thermal resistances connecting nodes C, H3 and Ambient, heat flow can also reverse in the bearing housing.

The oil temperature rises both as a result of heat transfer and frictional losses. It is assumed that heat is first exchanged by forced convection between nodes H1 and oil ($Q_{H1/Oil}$); secondly, the oil temperature rises due to frictional losses (W_m); Finally, further heat is transferred by forced convection with node H2 ($Q_{H2/Oil}$).

2.2 Model parameterisation

The turbocharger thermal model contains a number of parameters that are not easily determined by inspection of the geometry without considerable simplification (5 capacitances, 4 conductances and 7 convective correlations). Although an experimental procedure has been determined to characterise these parameters for an individual turbocharger, the aim of this work is to assess the predictive capability of the model for a new turbocharger, based on the parameters established previously for a similar device. A range of turbocharger sizes has previously been measured and simple correlations have been observed between external geometries and thermal parameters: these have been used to calculate the parameters in this study, this replicating an industrial scenario.

3 APPROACH

3.1 Experimental Setup and Test Points

A variable geometry turbocharger has been instrumented to capture fluid and structure temperatures at each of the locations described by the nodes of the model. For all gas temperatures, multiple thermocouples were used to capture distributions across the cross section of the ducts (figure 2a). For the compressor and turbine housings, temperatures were measured at 3 azimuths and 2 depths to provide information about temperature distributions (figure 2b). The turbocharger was installed on a 2.2L Diesel engine for which the usual application is a light commercial vehicle. The engine was operated on

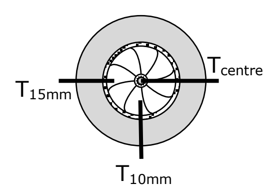

a) Gas temperature measurements in ducts

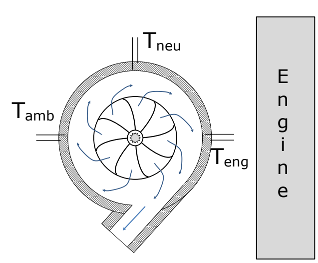

b) Compressor/Turbine Scroll

Figure 2: Thermal instrumentation of turbocharger

an AC transient dynamometer. Mass flow was measured at engine intake using an ABB Sensyflow hot wire flow meter (accuracy <1%); Pressures were measured using Kistler Piezo-Resistive sensors (accuracy 0.5%); gas and metal temperatures were measured using 1.5mm k-type thermocouples and turbocharger speed was measured using an eddy current blade count device from Micro-Epsillon.

The engine was operated over under thermally stable and transient conditions. These are shown with respect to the engine speed/torque map in figure 3 (a). For steady state tests, the engine was allowed to stabilise for 7 minutes before recording and measurements represent average behaviour over 60 seconds. The transient experiment consisted of a series of 32 step changes as shown in figure 3 (b) with a hold time of 3 minutes between steps; this tests is superimposed onto figure 3 (a) in grey.

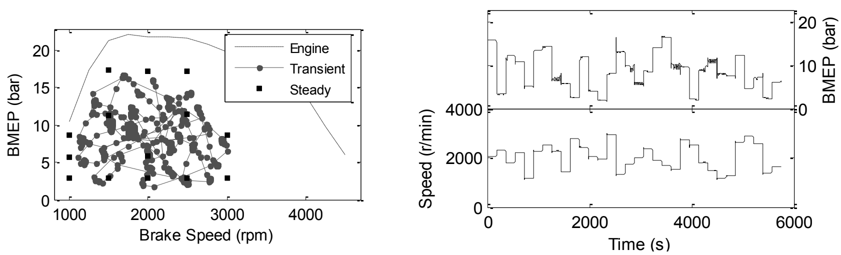

(a) *(b)*

Figure 3: Engine speed and torque operating points for stably and transient experiments (BMEP: Brake Mean Effective Pressure)

3.2 Model Control

One-dimensional simulation code OpenWAM™ (12, 13) has been used to create the turbocharger model with the connecting ducts as shown in figure 4. This highlights the compressor and turbine models (that are based on the manufacturer's maps) connected via a mechanical shaft and the lumped thermal model of the housing. The turbine map was determined from compressor enthalpy rise and is therefore adiabatic with respect to turbine performance, however this includes mechanical losses and was modified by applying the mechanical losses models developed by Serrano et al. (6, 14). The turbine is represented by a series of two nozzles with an intermediate reservoir to account for acoustic effects (15, 16).

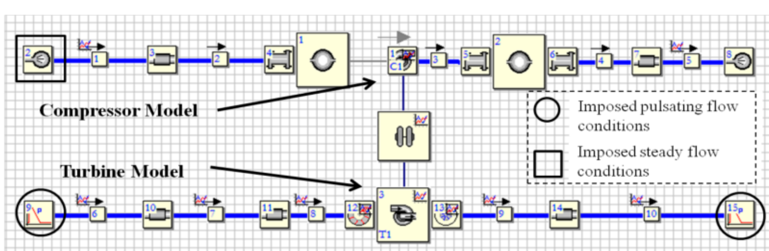

Figure 4: Turbocharger model boundary conditions for steady and transient simulations

To avoid inaccuracies of a full engine model, measured conditions have been imposed at the compressor and turbine inlets (pulsating pressure for turbine). A back-pressure valve has been introduced at compressor outlet to represent the flow restriction of the engine; the opening was tuned to give measured compressor mass flow at measured compressor speed. This approach was preferred to imposing compressor outlet pressure as it allows simulation errors to occur in pressure and mass flow. On turbine side outlet pressure was imposed and VGT position was tuned to match measured mass flow at measured turbine speed. For steady state the simulations were conducted in two phases:

1) The turbocharger was simulated at fixed speed whilst the flow coefficient of the orifice at compressor outlet and the turbine VGT positions were determined to match compressor and turbine flows respectively.
2) The VGT position and compressor outlet orifice were fixed based on the results from 1; the turbocharger speed was now calculated from the compressor and turbine power balance.

For the transient experiments, the PID approach is no longer possible as the dynamics of the controller would interfere with the physical dynamics. To avoid this problem look up tables were derived from the steady state data and interrogated via interpolation during transient simulations.

4 RESULTS

4.1 Steady State Conditions

The model accuracy with and without heat transfer simulation are compared in table 1. In terms of the turbocharger operating speed, pressure ratio and mass flow predictions there is no significant change in the accuracy of the simulation by adding the thermal model. Turbine outlet temperature prediction is improved somewhat with the RMSE reducing from 29°C to 13°C whilst compressor outlet temperature prediction remains similar. The thermal model allows a number of additional temperatures to be estimated: notably the oil temperature rise in the turbocharger and housing temperatures to within 10-17°C. The oil temperature rise Includes both friction and forced convective heat transfers. For the housings, previous studies by Romagnoli and Martinez-Botas (5) have shown that the temperature can vary locally by more than the model accuracy when operated on-engine; therefore discrepancies may be a result thermocouple installation.

Table 1: Root Mean Square Error (RMSE) for steady and transient simulations, with and without heat transfer (HT) model

Factor	Steady State		Transient State	
	HT OFF	**HT ON**	**HT OFF**	**HT ON**
Turbocharger Speed	4.0%	5.0%	2.7%	2.3%
Compressor pressure Ratio	3.1%	4.5%	5.1%	4.7%
Compressor Mass Flow	2.4%	3.1%	6.1%	6.0%
Compressor Outlet Temperature	7°C	8.4°C	11°C	10°C
Compressor Housing Temperature	N/A	17°C	N/A	12°C
Turbine Pressure Ratio	*Imposed*			
Turbine Mass Flow	2.3%	2.3%	4.2%	4.3%
Turbine Outlet Temperature	29°C	13°C	35°C	14°C
Turbine Housing Temperature	N/A	13°C	N/A	15°C
Oil Outlet temperature	N/A	9°C	N/A	7°C
Bearing Housing Temperature	N/A	11°C	N/A	16°C

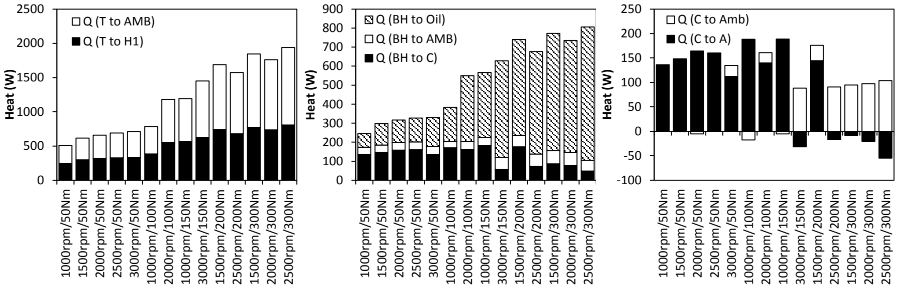

(a) Node T *(b) Nodes H1/H2/H3* *(c) Node C*

Figure 5: Predicted heat flows in selected turbocharger nodes

A breakdown of thermal energy flows between selected model nodes is given in figure 5; heat flows are presented for each node against engine operating point, ranked as increasing engine power. Considering first node T (figure 5a), the total heat transfer from exhaust gases increases with torque and power, with more than half this heat transferring to ambient. The central bearing housing node (figure 5b) shows that higher heat flow from the turbine housing is primarily absorbed into the oil. At higher engine powers, the heat flow to the compressor housing reduces which is also highlighted by the reversal of heat flow between air and compressor housing shown in figure 5c.

During the simulation, small errors in the operating maps will be compounded as they will shift simulated speed, mass flow and pressure ratio. A number of possible sources for these errors are: engine installation effects, operation under pulsating flows and manufacturing tolerances. Figure 6 shows the proportions of temperature change attributable to work and heat transfer: it is therefore unrealistic to assume that all simulation errors could be corrected by the heat transfer model.

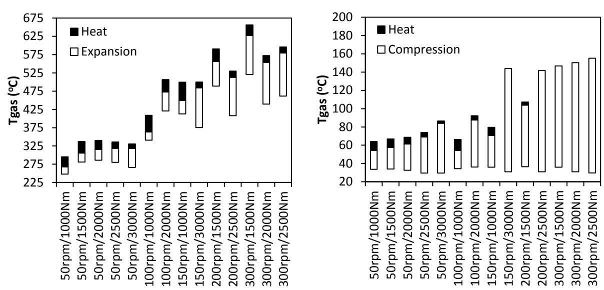

(a) Turbine *(b) Compressor*

Figure 6: Temperature changes due to compression/expansion and heat transfer for (a) turbine and (b) compressor

A sensitivity study was conducted to quantify the influence of each parameter in table 2. Based on the results in figure 7, the following observations are made:

- **Turbine Internal convection** has a direct effect on the heat flux between the gas and the housing (20-30%). This is not directly proportional to heat transfer coefficient because node T varies ±20-80°C whilst outlet gas temperature varied up to ±8°C. Heat flow through nodes H1, H2 and H3 is affected causing changes in node C of ±2°C, but less than 1°C change in compressor outlet temperature.

Table 2: Ranges of sensitivity tested

Factor	Variable	Variation	
Turbine Internal convection	$hA_{GAS/T}$ (eq 2)	-50%	+50%
Compressor internal convection	$hA_{C/AIR}$ (eq 2)	-50%	+50%
External Heat transfer	$hA_{X/AMB}$ (eq 2)	0	+100%
Internal Conduction	$K_{X/Y}$ (eq 1)	-50%	+50%

- **Compressor Internal Convection** caused variation in compressor outlet gas temperature and compressor housing of up to ±4°C. No significant effect on turbine temperatures was observed.
- **External Heat Transfer** had a significant influence on all four temperatures with gas temperatures and metal temperature varying ±2-14°C and ±5-80°C respectively.
- **Internal Conduction** controls the amount of heat conducting between the turbine and compressor housing. The sensitivity showed a ±19°C and ±7°C variation in turbine and compressor housing respectively and ±4°C and ±3°C in compressor and turbine gas outlet temperature respectively.

The study shows that the turbine behaviour is independent of compressor heat transfer, but that the opposite is not true. Metal temperatures are more sensitive to model parameters than gas temperatures, especially at high engine powers (with high compression/expansion ratios). The crucial influence of internal conduction for estimating metal temperatures demonstrates the need for a rigorous identification

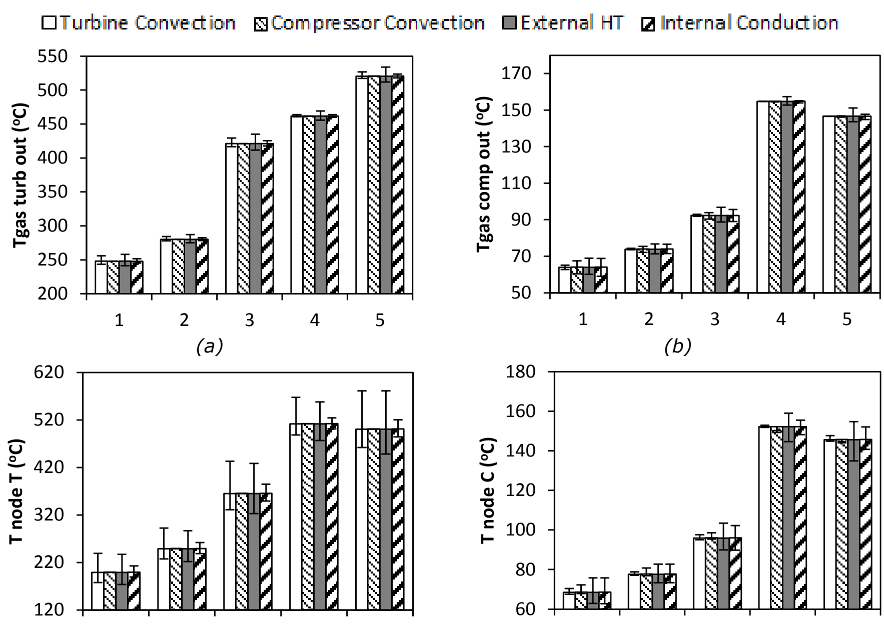

(a) (b) (c) (d)
1 – 50Nm/1000rpm 2 – 50Nm/2500rpm 3 – 100Nm/2000rpm
4 – 300Nm/2500rpm 5 – 300Nm/1500rpm

Figure 7: Model sensitivity to model parameters for (a) turbine gas outlet, (b) compressor gas outlet, (c) Node T and (d) Node C (Axis refers to different operating conditions, HT: Heat Transfer)

whilst the significant effect of external heat transfer highlights the need for accurate control and modelling of this. Nevertheless, the use here of the heat transfer model using parameters with high uncertainty has shown improved prediction of turbine outlet gas temperature.

4.2 Transient conditions

The prediction performance of the "best estimate" model over transient events is given in table 1 and compared graphically to measured results in figure 8. Overall the prediction is of similar accuracy to steady state performance, however under these conditions in addition to the parameters discussed above, the thermal capacity of each node is also important. A sensitivity analysis has also been carried out where thermal capacity was varied ±50%: figure 8 shows the results over a particular step in engine operating point from 280Nm/2000rpm to 60Nm/2300rpm. As the engine power is reduced, there is a rapid drop in compressor and turbine outlet temperature associated with the expansion and compression processes. Subsequently a much slower temperature reduction is observed, associated with heat transfer and thermal inertia. On the turbine side, ±50% in housing thermal capacity resulted in ±20-40°C and ±8-11°C in metal and gas temperature prediction over the transient; on the compressor theses were ±7°C and ±4°C respectively.

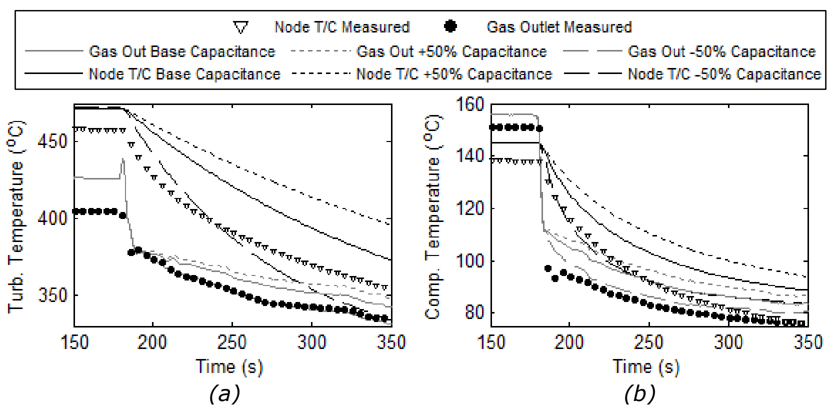

Figure 8: Model sensitivity to thermal capacitance for (a) turbine and (b) compressor

5 CONCLUSIONS

A study of the predictive performance of a turbocharger heat transfer model has been undertaken under steady and transient conditions. This showed that turbine outlet temperature prediction RMSE could be reduced from 29 to 13°C for steady state conditions whilst other predictions were of similar accuracy. The model allowed metal temperature to be estimated to within 17°C and 15°C for compressor and turbine housings respectively. A sensitivity study showed that uncertainty in the model parameters could affect gas temperatures up to ±4°C and metal temperatures up to 80°C. Under transient events, the uncertainty associated with thermal capacity of the nodes increases the errors but this has limited influence on gas temperatures. The results show that at this stage it is possible to improve the prediction of turbine outlet temperature on-engine by using the heat transfer model and inferring properties from a similar device. However the sensitivity study has suggested that a further accuracy improvement would be expected if a full thermal characterisation was undertaken.

REFERENCES

[1] M. Cormerais, J. F. Hetet, P. Chesse, and A. Maiboom, Heat Transfer Analysis in a Turbocharger Compressor: Modeling and Experiments, SAE Paper Number 2006-01-0023, 2006.

[2] J. R. Serrano, C. Guardiola, V. Dolz, A. Tiseira, and C. Cervelló, Experimental Study of the Turbine Inlet Gas Temperature Influence on Turbocharger Performance, SAE Paper Number 2007-01-1559, 2007.

[3] S. Shaaban, Experimental investigation and extended simulation of turbocharger non-adiabatic performance, PhD, Fachbereich Maschinenbau, Universität Hannover, 2004.

[4] N. Baines, K. D. Wygant, and A. Dris, The analysis of heat transfer in automotive turbochargers, *Journal of Engineering for Gas Turbines and Power,* vol. 132(4), 2010.

[5] A. Romagnoli and R. Martinez-Botas, Heat transfer analysis in a turbocharger turbine: An experimental and computational evaluation, *Applied Thermal Engineering,* vol. 38, pp. 58-77, 2012.

[6] J. R. Serrano, P. Olmeda, A. Tiseira, L. M. Garcia-Cuevas, and A. Lefebvre, Theoretical and experimental study of mechanical losses inautomotive turbochargers, *Energy,* vol. 55, pp. 888-898, 2013.

[7] M. Cormerais, P. Chesse, and J.-F. Hetet, Turbocharger heat transfer modeling under steady and transient conditions, *International Journal of Thermodynamics,* vol. 12, pp. 193-202, 2009.

[8] P. Olmeda, V. Dolz, F. J. Arnau, and M. A. Reyes-Belmonte, Determination of heat flows inside turbochargers by means of a one dimensional lumped model, *Mathematical and Computer Modelling,* vol. 57, pp. 1847-1852, 2013.

[9] J. R. Serrano, P. Olmeda, A. Paez, and F. Vidal, An experimental procedure to determine heat transfer properties of turbochargers, *Measurement Science & Technology,* vol. 21, Mar 2010.

[10] S. Shaaban, J. R. Seume, R. Berndt, H. Pucher, and H. J. Linnhoff, Part Load performance prediction of turbocharged engines, presented at the 8th International Conference on Turbochargers and Turbocharging, May 17, 2006 - May 18, 2006, London, United kingdom, 2006.

[11] F. Payri, P. Olmeda, F. J. Arnau, A. Dombrovsky, and L. Smith, External heat losses in small turbocharger: model and experiments, *Submitted to Energy,* 2013.

[12] *OpenWAM*, 2012. Available: www.Openwam.org

[13] J. Galindo, J. R. Serrano, F. J. Arnau, and P. Piqueras, Description of a Semi-Independent Time Discretization Methodology for a One-Dimensional Gas Dynamics Model, *Journal of Engineering for Gas Turbines and Power-Transactions of the Asme,* vol. 131, May 2009.

[14] J. R. Serrano, P. Olmeda, A. Tiseira, L. M. García-Cuevas, and A. Lefebvre, Importance of Mechanical Losses Modeling in the Performance Prediction of Radial Turbochargers under Pulsating Flow Conditions, *SAE Int. J. Engines,* vol. 6, pp. 729-738, 2013.

[15] J. R. Serrano, F. J. Arnau, V. Dolz, A. Tiseira, and C. Cervelló, A model of turbocharger radial turbines appropriate to be used in zero- and one-dimensional gas dynamics codes for internal combustion engines modelling, *Energy Conversion and Management,* vol. 49, pp. 3729-3745, 2008.

[16] M. A. Reyes-Belmonte, Contribution to the Experimental Characterization and 1-D Modelling of Turbochargers for IC Engines, PhD, Departamento de Máquinas y Motores Térmicos, Universitat Politècnica de València, València, 2013.